Journal of Power Sources 195 (2010) 3661–3667

Contents lists available at ScienceDirect

Journal of Power Sources

journal homepage: www.elsevier.com/locate/jpowsour

Synthesis of carbon-coated $LiFePO_4$ nanoparticles with high rate performance in lithium secondary batteries

Muxina Konarova, Izumi Taniguchi*

Department of Chemical Engineering, Graduate School of Science and Engineering, Tokyo Institute of Technology, 2-12-1 Ookayama, Meguro-ku, Tokyo 152-8552, Japan

ARTICLE INFO

Article history:
Received 12 October 2009
Accepted 5 November 2009
Available online 8 January 2010

Keywords:
Carbon-coated $LiFePO_4$
Nanoparticles
Spray pyrolysis
Wet ball milling
Lithium-ion batteries
Cathode

ABSTRACT

A novel preparation technique was developed for synthesizing carbon-coated $LiFePO_4$ nanoparticles through a combination of spray pyrolysis (SP) with wet ball milling (WBM) followed by heat treatment. Using this technique, the preparation of carbon-coated $LiFePO_4$ nanoparticles was investigated for a wide range of process parameters such as ball-milling time and ball-to-powder ratio. The effect of process parameters on the physical and electrochemical properties of the $LiFePO_4$/C composite was then discussed through the results of X-ray diffraction (XRD) analysis, field-emission scanning electron microscopy (FE-SEM), transmission electron microscopy (TEM), the Brunauer–Emmet–Teller (BET) method and the use of an electrochemical cell of Li|1 M $LiClO_4$ in EC:DEC = 1:1|$LiFePO_4$. The carbon-coated $LiFePO_4$ nanoparticles were prepared at 500 °C by SP and then milled at a rotating speed of 800 rpm, a ball-to-powder ratio of 40/0.5 and a ball-milling time of 3 h in an Ar atmosphere followed by heat treatment at 600 °C for 4 h in a N_2 + 3% H_2 atmosphere. SEM observation revealed that the particle size of $LiFePO_4$ was significantly affected by the process parameters. Furthermore, TEM observation revealed that the $LiFePO_4$ nanoparticles with a geometric mean diameter of 146 nm were coated with a thin carbon layer of several nanometers by the present method. Electrochemical measurement demonstrated that cells containing carbon-coated $LiFePO_4$ nanoparticles could deliver markedly improved battery performance in terms of discharge capacity, cycling stability and rate capability. The cells exhibited first discharge capacities of 165 mAh g^{-1} at 0.1 C, 130 mAh g^{-1} at 5 C, 105 mAh g^{-1} at 20 C and 75 mAh g^{-1} at 60 C with no capacity fading after 100 cycles.

1. Introduction

$LiFePO_4$ has recently received much attention owing to its potential use as a next-generation cathode material in lithium-ion batteries because of its relative lack of toxicity and the low cost and abundance of its raw materials. It also has a high lithium intercalation voltage of 3.4 V compared with lithium metal and a high theoretical capacity of 170 mAh g^{-1} [1,2]. However, olivine $LiFePO_4$ has a low electronic conductivity and a low lithium diffusivity [1,3–6] which prevent its large-scale application in electric vehicles (EVs) and hybrid electric vehicles (HEVs). The poor rate capability of $LiFePO_4$ cathodes makes it difficult to make full use of them in lithium-ion batteries unless modifications are made to improve their low electronic conductivity and the slow lithium ion diffusion across the $LiFePO_4$/$FePO_4$ interface. Thus far, much effort has been made to improve the electrochemical properties of $LiFePO_4$ by reducing the particle size [6–11] and coating $LiFePO_4$ particles with carbon [12–19] or a $LiFePO_4$/C composite [4,20–26]. Furthermore, various synthesis methods have been developed to prepare $LiFePO_4$ materials, involving solid-state reactions [5,18,21,27–29], the polyol process [7], the sol–gel process [29,30], hydrothermal synthesis [12,29,31,32], microwave synthesis [3,12,20,33], the solvothermal method [11,34], mechanical activation [6,13,14,16,17,24,35–37], coprecipitation [8,9] and the template method [22,38,39]. However, as a result, the synthesis procedure has become more complicated, particularly when a reduced particle size and a carbon coating of $LiFePO_4$ are required. The majority of the above synthesis methods require high annealing temperatures, long annealing times or several grinding steps. It is also difficult to precisely control the chemical composition of the as-prepared materials in the case of hydrothermal synthesis.

Spray pyrolysis (SP) is a well-known continuous and single-step method for the preparation of fine homogeneous and multicomponent powders. Compared with particles obtained by conventional ceramic preparation methods, those obtained by SP exhibit a particle size distribution that is narrow and controllable from micrometer to submicrometer order, high purity and ease of composition control [40]. Even if the post-annealing of as-prepared powders by SP is required to obtain the desired materials, a shorter annealing time of the as-prepared powders may be necessary in

* Corresponding author. Tel.: +81 3 5734 2155; fax: +81 3 5734 2155.
E-mail address: taniguchi.i.aa@m.titech.ac.jp (I. Taniguchi).

0378-7753/$ – see front matter.
doi:10.1016/j.jpowsour.2009.11.147

SP than in conventional ceramic preparation methods. Moreover, as-milled powders with a narrow particle size distribution can be obtained after ball-milling the as-prepared powders obtained by SP. In contrast, several long sintering and regrinding procedures are needed to obtain the final product by a solid-state reaction [27,28], and the final powders may have a wide particle size distribution. Recently, Kang and Ceder [28] have reported the ultrahigh rate capability of $LiFe_{0.9}P_{0.95}O_{4-\delta}$ prepared by a solid-state reaction. However, Zaghib et al. [41] have extensively questioned their results.

In our previous studies [4,17], a $LiFePO_4$/C composite and a carbon-coated $LiFePO_4$ particles were prepared by SP and a combination of SP with dry ball milling (DBM), respectively. It could be clearly seen in those studies that the use of the carbon composite and coating is an effective approach to improving the electrochemical properties of the $LiFePO_4$ cathode material. However, the electrochemical performance of the prepared materials was not satisfactory for large-scale application in EVs and HEVs because the size of $LiFePO_4$ particles was approximately 300 nm [17]. The reduction in particle size is also a key factor for obtaining $LiFePO_4$ with a high rate capability. Thus, we develop a novel preparation technique for carbon-coated $LiFePO_4$ nanoparticles in this work.

2. Experimental

2.1. Preparation of carbon-coated $LiFePO_4$ nanoparticles

The precursor solution was prepared by dissolving the correct amounts of $Li(HCOO)\cdot H_2O$, $FeCl_2\cdot 4H_2O$ and H_3PO_4 in distilled water in a stoichiometric ratio. The concentrations of Li^+, $Fe^{2+}$and PO_4^{3-} were all 0.2 mol dm^{-3}. The pH of the precursor solution was adjusted to 1.9 by adding HCl.

A schematic diagram of the SP setup was provided in our previous paper [42]. The precursor solution was atomized at a frequency of 1.7 MHz using an ultrasonic nebulizer. The sprayed droplets were transported to the reactor by N_2 gas. The flow rate of N_2 gas was 1 dm^3 min^{-1} and the reactor temperature was fixed at 500 °C [4]. The as-prepared $LiFePO_4$ powder was milled using a planetary ball mill (P-7, FRITSCH) in Ar atmosphere. To avoid $LiFePO_4$ particle growth during heat treatment [17], the as-prepared $LiFePO_4$ powder was mixed with acetylene black at a weight ratio of 90:10 in the WBM process. Ethanol was used as a medium. Zirconia balls and a 45 ml zirconia vial were also used during WBM. The ball-to-powder weight ratio was varied from 40/1 to 40/0.3 and the rotating speed was fixed at 800 rpm. The ball-milling time was also varied from 1 to 12 h. After the ball milling, the samples were heated at 600 °C for 4 h in a N_2 + 3% H_2 atmosphere in a tubular furnace [4]. Fig. 1 shows a flowchart for the preparation of carbon-coated $LiFePO_4$ nanoparticles.

2.2. Sample characterization

The crystalline phase of the samples was identified by X-ray diffraction (XRD, Ultima IV with D/teX Ultra, Rigaku) using Cu Kα radiation. The lattice parameters were determined by the Rietveld refinement of the XRD patterns using the software package PDXL (Rigaku, Ver. 1.3.0.0). The particle size and morphology of the samples were examined by field-emission scanning electron microscopy (FE-SEM, S-800, Hitachi) and transmission electron microscopy (TEM, JEM-200CX, JEOL). The geometric mean diameter $d_{g,p}$ and geometric standard deviation σ_g were determined by randomly sampling approximately 500 particles from the TEM images. The specific surface area was determined by the Brunauer–Emmet–Teller method (BET, Flow Sorb II 2300, Shimadzu). The carbon content of the products was analyzed using an element analyzer (CHN corder MT-6, YANACO).

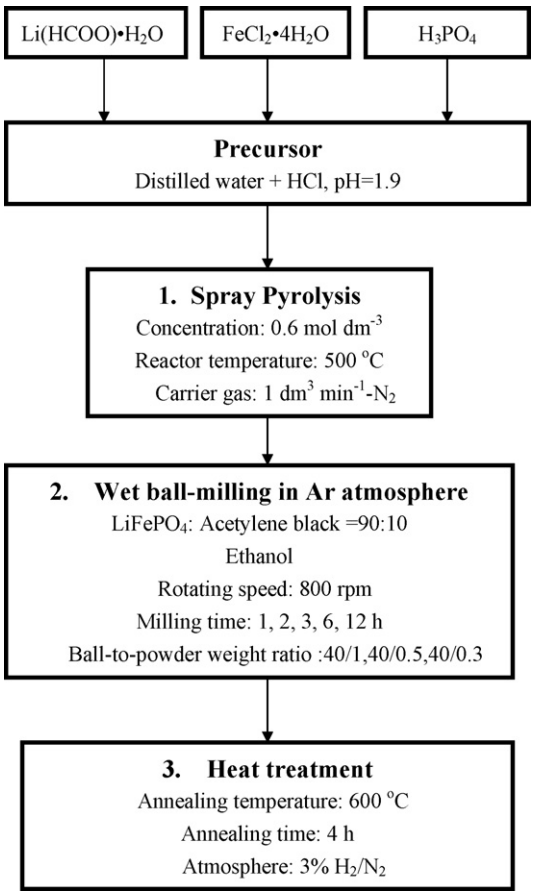

Fig. 1. Flowchart for the preparation of carbon-coated $LiFePO_4$ nanoparticles by the combination of SP with WBM followed by heat treatment.

2.3. Fabrication of electrochemical cells and electrochemical characterization

Electrochemical characterization was performed by assembling a CR2032 coin cell for galvanostatic charge–discharge testing. The cell comprised a lithium metal electrode and a $LiFePO_4$ electrode separated by a microporous polypropylene separator. 1 M $LiClO_4$ in EC:DEC = 1:1 (Tomiyama Pure Chemical Co., Ltd.) was used as the electrolyte. The cathode consisted of 70 wt.% $LiFePO_4$, 10 wt.% polyvinylidene fluoride (PVDF) as a binder and 20 wt.% acetylene black. These materials were dispersed in 1-methyl-2-pyrrolidinone (NMP), and the resultant slurry was then spread onto an aluminum foil using the doctor blade technique. The coated aluminum foil was dried for 4 h in an oven set at 110 °C and then pressed to achieve good adherence between the coated material and the aluminum foil. The cathode was formed by punching a circular disc from the foil and scraping it to standardize the area of the cathode (100 mm^2). The coin cell was assembled inside a glove box filled with high-purity argon gas (99.9995% purity). The cell was cycled galvanostatically between 2.5 and 4.3 V using multichannel battery testers (HJ1010mSM8A, Hokuto Denko) at various charge–discharge rates ranging from 0.1 to 60 C at room temperature.

3. Results and discussion

3.1. Effects of ball-milling time and ball-to-powder ratio on the physical properties of $LiFePO_4$/C composite

Fig. 2 shows XRD patterns of the $LiFePO_4$/C composite samples synthesized by SP and then milled at a ball-to-powder ratio of

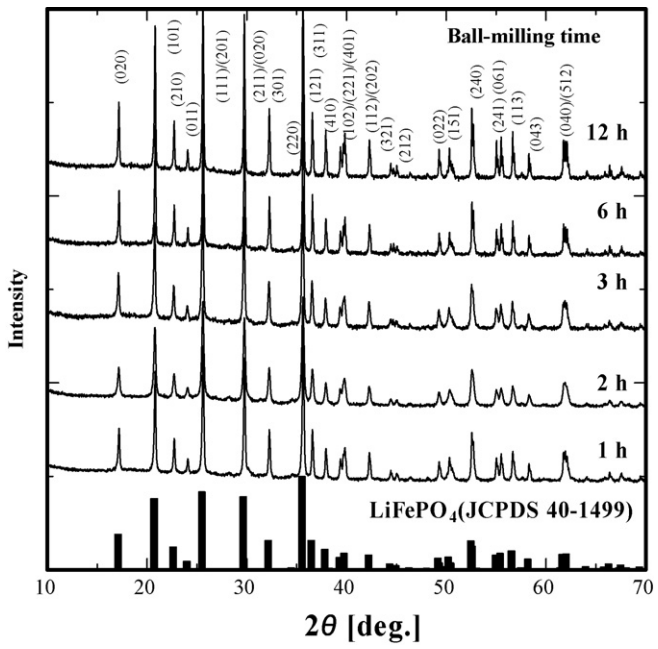

Fig. 2. XRD patterns of the $LiFePO_4$/C composite samples prepared by the combination of SP with WBM for various times in an Ar atmosphere followed by heat treatment. Ball-to-power ratio: 40/0.5.

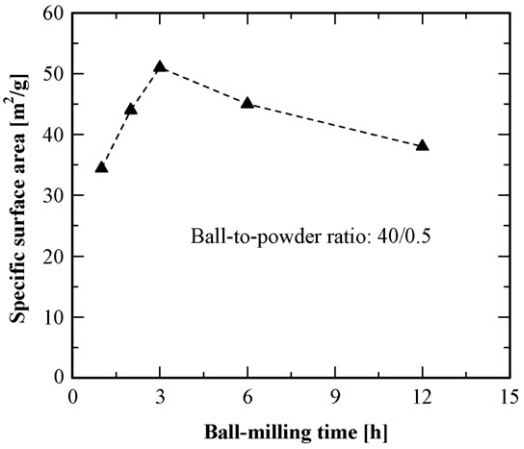

Fig. 3. Variation of the specific surface area of $LiFePO_4$/C composite samples with ball-milling time. Ball-to-power ratio: 40/0.5.

40/0.5 for various ball-milling times from 1 to 12 h followed by heat treatment. The JCPDS standard $LiFePO_4$ patterns are also shown in the figure. The diffraction peaks of all the samples are identified as those of the orthorhombic structure with the space group *Pnma* without any secondary phases such as Fe_2P and Fe_3P. The results of the Rietveld refinement are summarized in Table 1. Satisfactory and acceptable statistical fit values ($S = R_{wp}/R_p$) are obtained. The lattice parameters and unit cell volumes obtained for the synthesized samples after various ball-milling times are in good agreement with those reported earlier for the *Pnma* structure [1,4,13,36].

We have already reported that the electrochemical properties of $LiFePO_4$ are strongly affected by the specific surface area, and that a $LiFePO_4$ sample with a larger specific surface area shows better electrochemical performance [4]. Thus, the effect of process parameters such as ball-milling time and ball-to-powder ratio on the specific surface area of the $LiFePO_4$ samples was investigated.

Fig. 3 shows the variation of the specific surface area of the $LiFePO_4$/C composite samples with ball-milling time. The samples were synthesized by SP and then ball-milled at a ball-to-powder ratio of 40/0.5 for various times from 1 to 12 h followed by heat treatment. The specific surface area considerably increases with ball-milling time up to 3 h. However, a further increase in ball-milling time results in a gradual decrease in the specific surface area. This fact suggests that both the milling and agglomeration of $LiFePO_4$ and acetylene black powders occurred during WBM. To clarify the effect of ball-milling time on the specific surface area, the powder morphology of the samples was also observed by SEM. Fig. 4 shows the result. For comparison, an SEM image of the $LiFePO_4$/C composite prepared at 500 °C by SP and then sintered at 600 °C for 4 h in a N_2 + 3% H_2 atmosphere is also shown in the figure. $LiFePO_4$ powder with particle sizes of 1–3 μm was synthesized by SP followed by heat treatment, while $LiFePO_4$ powder with particle sizes of 300–500 nm was prepared by WBM for 3 h. However, undesired particle agglomeration occurred upon increasing the ball-milling time from 3 to 12 h.

Fig. 5 shows XRD patterns of $LiFePO_4$/C composite samples synthesized by SP and then ball-milled for 3 h at various ball-to-powder ratios from 40/1 to 40/0.3 followed by heat treatment. The XRD patterns also show a single-phase olivine structure. The lattice parameters and unit cell volumes of the synthesized samples for various ball-milling times are also given in Table 1. These values closely match data in the literature [1,4,13,36].

Fig. 6 shows the effect of ball-to-powder ratio on the specific surface area of the $LiFePO_4$/C composite samples. The samples were synthesized by SP and then milled for 3 h at various ball-to-powder ratios from 40/1 to 40/0.3 followed by heat treatment. As the rotating speed and amount of zirconia balls were fixed at 800 rpm and 40 g, respectively, the milling energy per weight of powder increases with decreasing amount of powder. The specific surface area was found to gradually increases with the ball-to-powder ratio. However, it reaches a maximum at a ball-to-powder ratio of 40/0.5 and then deceases with increasing ball-to-powder ratio. This may be due to the reduced collision frequency among the zirconia balls and the $LiFePO_4$ and acetylene black powder particles in the case of using a too small amount of powder, which may decrease the actual milling energy given to the powder.

From the above-mentioned results, we can conclude that the $LiFePO_4$/C composite with the largest specific surface area can be prepared by a combination of SP at 500 °C with WBM for 3 h at a

Table 1
Lattice parameters and Rietveld coefficients of the samples.

Preparation conditions		*a* [Å]	*b* [Å]	*c* [Å]	*V* [Å³]	$S = R_{wp}/R_p$
Milling time [h]	Ball-to-powder ratio					
1	80(40/0.5)	10.3306	6.0064	4.6933	291.218	1.6434
2	80(40/0.5)	10.3317	6.0047	4.6945	291.241	1.6163
3	40(40/1)	10.3256	6.0036	4.6928	290.910	1.6388
3	80(40/0.5)	10.3268	6.0051	4.6913	290.924	1.1416
3	133(40/0.3)	10.3242	6.0017	4.6955	290.946	1.5385
6	80(40/0.5)	10.3302	6.0066	4.6911	291.080	1.1689
12	80(40/0.5)	10.3311	6.0070	4.6915	291.149	1.3933

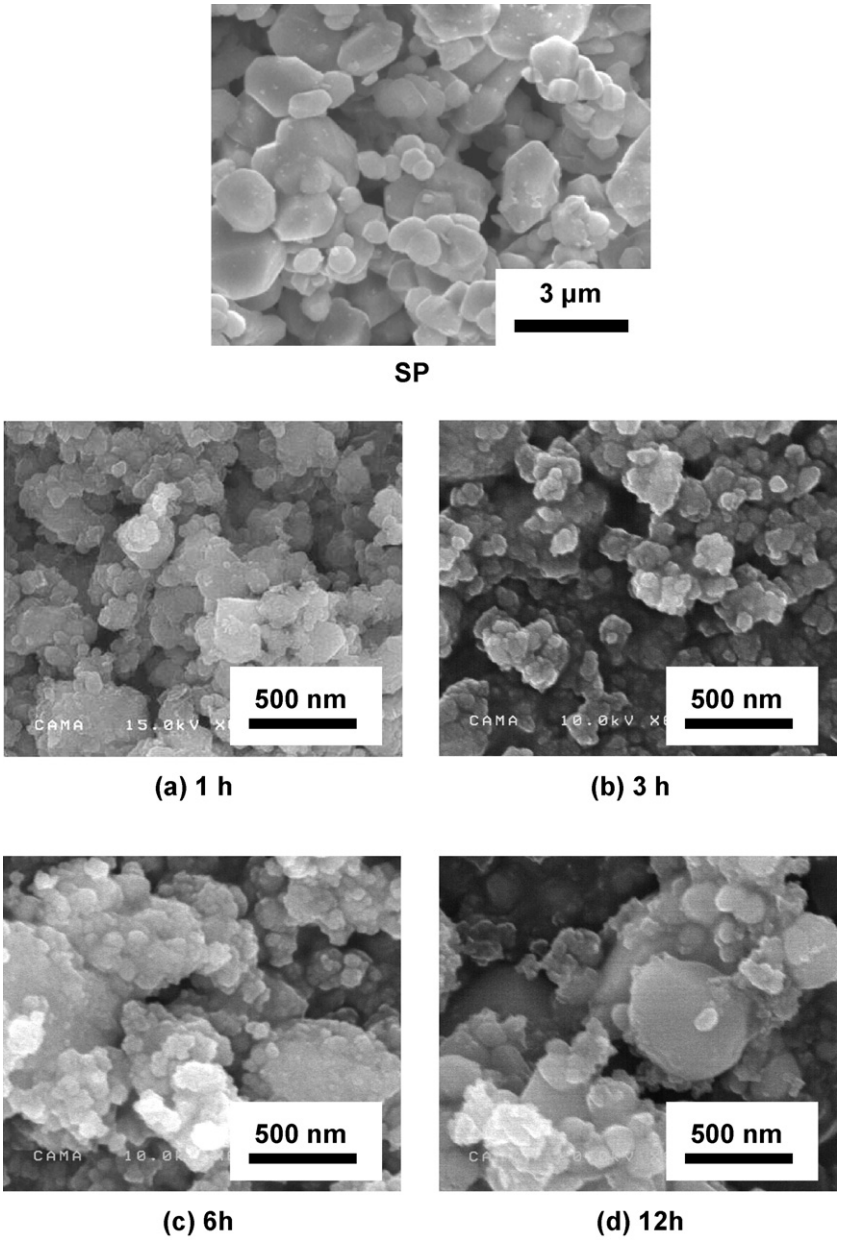

Fig. 4. SEM images of the $LiFePO_4$/C composite samples prepared by the combination of SP with WBM for various times followed by heat treatment. Ball-to-power ratio: 40/0.5.

ball-to-powder ratio of 40/0.5 followed by heat treatment at 600 °C for 4 h in a N_2 + 3% H_2 atmosphere.

To determine the particle size and distribution of this sample, TEM was used. Fig. 7a shows TEM images and the particle size distribution of the sample. The powder was composed of primary particles with size of a few hundreds of nanometers that were slightly agglomerated. From the TEM images, geometric mean diameter and geometric standard deviation were determined by randomly sampling approximately 500 particles, and their values for the powder were $d_{g,p}$ = 146 nm and σ_g = 1.4, respectively. However, the low-magnification TEM image gave little information on the composite structure between $LiFePO_4$ and carbon. Thus, a high-magnification TEM image of the obtained composite structure of the sample is shown in Fig. 7b. An amorphous carbon layer with a thickness in the range of 5–20 nm is formed on the surface of $LiFePO_4$ nanoparticles. It can be seen from the figure that carbon-coated $LiFePO_4$ nanoparticles with a uniform particle size distribution were synthesized by the present method. We conclude that carbon-coated $LiFePO_4$ nanoparticles can be prepared by a combination of SP at 500 °C with WBM for 3 h at a ball-to-powder ratio of 40/0.5 followed by heat treatment at 600 °C for 4 h in a N_2 + 3% H_2 atmosphere.

To confirm the carbon content of all the $LiFePO_4$/C composite samples, the CHN analysis was conducted, and results showed good agreement in carbon content between the samples and the starting material in WBM.

3.2. *Effects of ball-milling time and ball-to-powder ratio on electrochemical properties of $LiFePO_4$/C composite*

The effects of ball-milling time on the first discharge capacity of the $LiFePO_4$/C composite samples at charge–discharge rate of 0.1 and 10 C are shown in Fig. 8. The ball-to-powder ratio is 40/0.5. The first discharge capacity of the sample at 0.1 C increases with

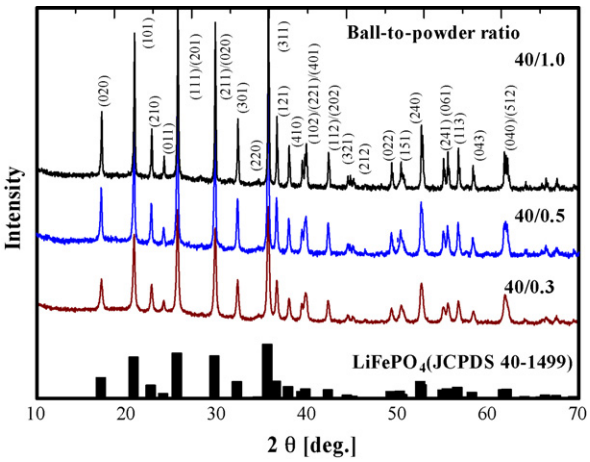

Fig. 5. XRD patterns of the $LiFePO_4$/C composite samples prepared by the combination of SP with WBM for various ball-to-powder ratios followed by heat treatment. Ball-milling time: 3 h.

ball-milling time up to 3 h and reaches a maximum at 3 h. However, it then gradually decreases with increasing ball-milling time. This tendency becomes clear at 10 C. As shown in Fig. 3, the $LiFePO_4$ sample ball-milled for 3 h has the largest specific surface area. The correlation between ball-milling time and first discharge capacity corresponds to that between ball-milling time and specific surface area. The effects of ball-to-powder ratio on the first discharge capacity of the $LiFePO_4$ samples at charge–discharge rate of 0.1 and 10 C are shown in Fig. 9. A similar result was also obtained from the figure. These results suggest that for a $LiFePO_4$/C composite, the larger the specific surface area, the lager the discharge capacity. As a result, we were able to confirm that the electrochemical properties of the $LiFePO_4$/C composite prepared by the present method are clearly affected by the specific surface area of the sample.

3.3. Electrochemical properties of carbon-coated $LiFePO_4$ nanoparticles

The first charge–discharge profiles of cells containing carbon-coated $LiFePO_4$ nanoparticles with increasing charge–discharge rate from 0.1 to 60 C between 2.5 and 4.3 V are presented in Fig. 10. At a charge–discharge rate of 0.1 C, the cell has a discharge capacity of 165 mAh g^{-1}, which corresponds to 96% of the theoretical capacity of $LiFePO_4$ (170 mAh g^{-1}) and much smaller polarization loss

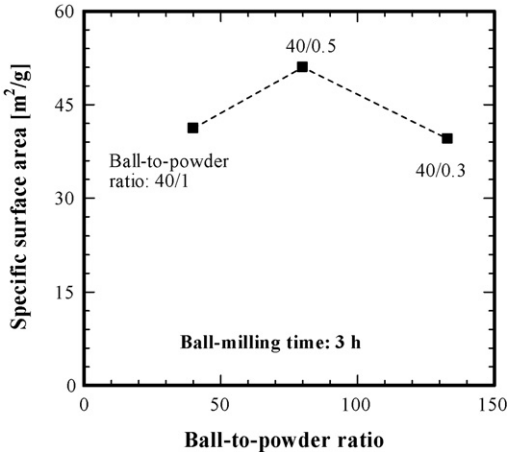

Fig. 6. Variation of the specific surface area of $LiFePO_4$/C composite samples with ball-to-powder ratio. Ball-milling time: 3 h.

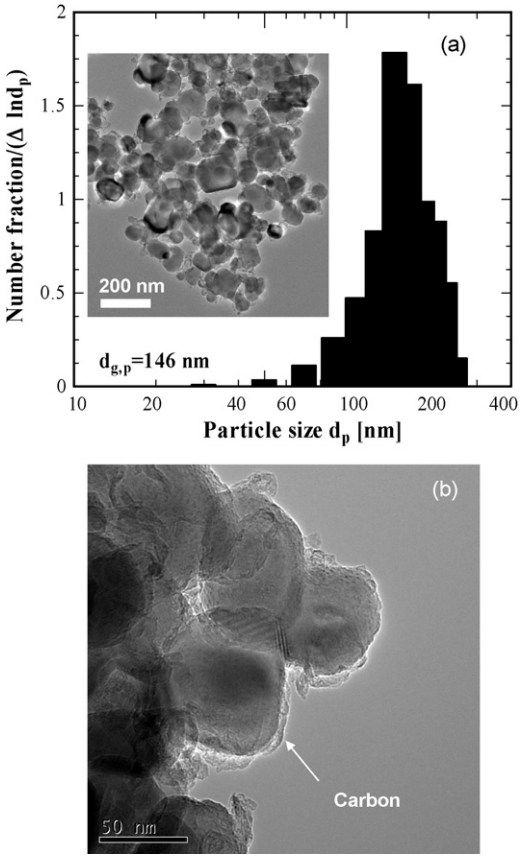

Fig. 7. TEM images and particle size distribution of the sample prepared by the combination of SP with WBM for 3 h at a ball-to-powder ratio of 40/0.5 followed by heat treatment.

and irreversible capacity. Furthermore, a wide flat voltage plateau is observed at 3.4 V, corresponding to the Fe^{+2}/Fe^{+3} redox reaction. The first discharge capacities at charge–discharge rates of 1, 5, 10, and 20 C are 155, 130, 118, and 105 mAh g^{-1}, respectively. Even at a charge–discharge rate of 60 C, the electrode containing carbon-coated $LiFePO_4$ nanoparticles has a discharge capacity of 75 mAh g^{-1}.

The cycle performance of the cells containing carbon-coated $LiFePO_4$ nanoparticles was investigated for up to 100 cycles at different charge–discharge rates, and the results are given in Fig. 11. The cells exhibit an excellent long-term cycling property. There is no capacity fading in the cells after 100 cycles at charge–discharge rates of 1 and 60 C. These results demonstrate that the structure of

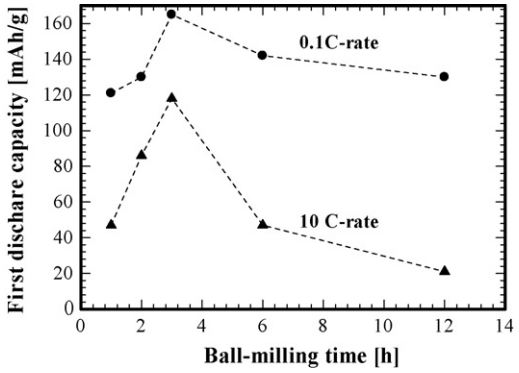

Fig. 8. Effect of ball-milling time on the first discharge capacity of the $LiFePO_4$/C composite prepared by the combination of SP with WBM followed by heat treatment. Ball-to-powder ratio: 40/0.5.

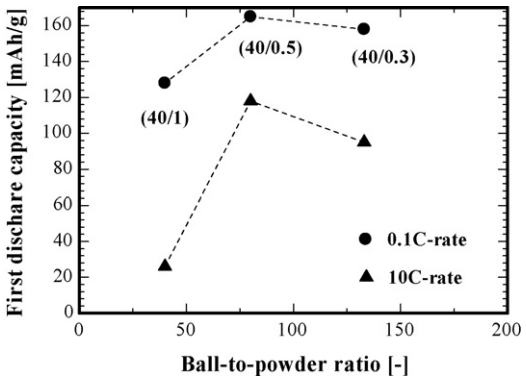

Fig. 9. Effect of ball-to-powder ratio on the first discharge capacity of the $LiFePO_4$/C composite prepared by the combination of SP with WBM followed by heat treatment. Ball-milling time: 3 h.

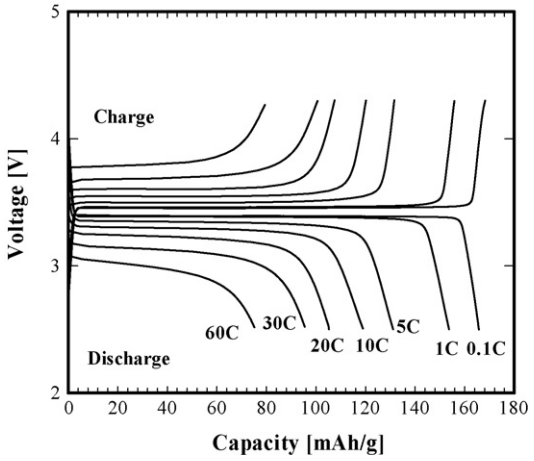

Fig. 10. First charge–discharge curves of the cells containing carbon-coated $LiFePO_4$ nanoparticles prepared by the combination of SP with WBM followed by heat treatment. Ball-milling time: 3 h. Ball-to-powder ratio: 40/0.5.

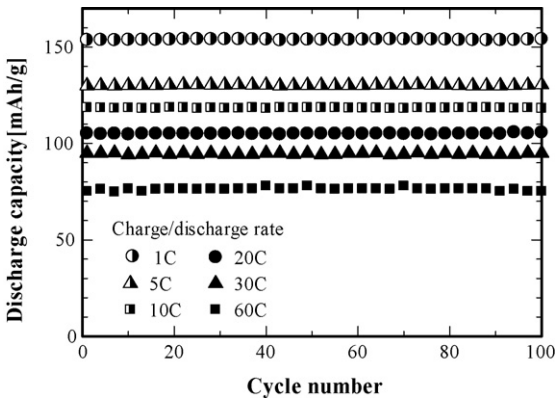

Fig. 11. Cycle performance of the cells containing carbon-coated $LiFePO_4$ nanoparticles prepared by the combination of SP with WBM followed by heat treatment. Ball-milling time: 3 h. Ball-to-powder ratio: 40/0.5.

the carbon-coated $LiFePO_4$ nanoparticles is very stable and that the electrochemical lithium-ion insertion/extraction process is quite reversible even at high charge–discharge rates. It is worth mentioning that the present preparation approach using the combination of SP with WBE followed by heat treatment enables us to achieve a high rate performance for $LiFePO_4$ composite electrode materials in lithium-ion batteries.

4. Conclusions

Carbon-coated $LiFePO_4$ nanoparticles were successfully prepared by a combination of SP with WBM at a rotating speed of 800 rpm and a ball-to-powder ratio of 40/0.5 for 3 h in an Ar atmosphere followed by heat treatment at 600 °C for 4 h in a N_2 + 3% H_2 atmosphere. The XRD patterns of the sample were assigned to an ordered olivine structure indexed by orthorhombic *Pnma*. TEM observation demonstrated that carbon-coated $LiFePO_4$ nanoparticles with a geometric mean diameter of 146 nm and a geometric standard deviation of 1.4 were obtained by the present method. The cells containing carbon-coated $LiFePO_4$ nanoparticles exhibited first discharge capacities of 165 mAh g^{-1} at 0.1 C and 105 mAh g^{-1} at 20 C. They also exhibited no capacity fading after 100 cycles at various charge–discharge rates from 1 to 60 C. These results clearly demonstrate that carbon-coated $LiFePO_4$ nanopaticles prepared by a combination of SP with WBM followed by heat treatment can be used as a cathode material of lithium-ion batteries for large-scale application in Plug-in HEVs and HEVs.

Acknowledgments

This research was partially supported by the Development of an Electric Energy Storage System for Grid-connection with New Energy Resources in New Energy and Industrial Technology Development Organization, the Nippon Sheet Glass Foundation for Materials Science and Engineering and the Yazaki Memorial Foundation for Science and Technology. The authors are grateful to the staff members of the Center for Advanced Materials Analysis (Tokyo Institute of Technology, Japan) for assistance in the TEM observation of carbon-coated $LiFePO_4$ nanoparticles.

References

[1] A.K. Padhi, K.S. Nanjundaswamy, J.B. Goodenough, J. Electrochem. Soc. 144 (1997) 1188.
[2] A.K. Padhi, K.S. Nanjundaswamy, C. Masquelier, S. Okada, J.B. Goodenough, J. Electrochem. Soc. 144 (1997) 1609.
[3] A.V. Murugan, T. Muraliganth, A. Manthiram, Electrochem. Commun. 10 (2008) 903.
[4] M. Konarova, I. Taniguchi, Mater. Res. Bull. 43 (2008) 3305.
[5] Y.-D. Cho, G.T.-K. Fey, H.-M. Kao, J. Power Sources 189 (2009) 256.
[6] J.-K. Kim, G. Cheruvally, J.-W. Choi, J.-U. Kim, J.-H. Ahn, G.-B. Cho, K.-W. Kim, H.-J. Ahn, J. Power Sources 166 (2007) 211.
[7] D.-H. Kim, J. Kim, Electrochem. Solid-State Lett. 9 (2006) A439.
[8] G. Arnold, J. Garche, R. Hemmer, S. Strobele, C. Vogler, M. Wohlfahrt-Mehrens, J. Power Sources 119-121 (2003) 247.
[9] C. Delacourt, P. Poizot, S. Levasseur, C. Masquelier, Electrochem. Solid-State Lett. 9 (2006) A352.
[10] P. Gibot, M. Casas-Cabanas, L. Laffont, S. Levasseur, P. Carlach, S. Hamelet, J.-M. Tarason, C. Masquelier, Nat. Mater. 7 (2008) 741.
[11] K. Saravanan, M.V. Reddy, P. Balaya, H. Gong, B.V.R. Chowdari, J.J. Vittal, J. Mater. Chem. 19 (2009) 605.
[12] A.V. Murugan, T. Muraliganth, A. Manthiram, J. Electrochem. Soc. 156 (2009) A79.
[13] K. Zaghib, A. Mauger, F. Gendron, C.M. Julien, Chem. Mater. 20 (2008) 462.
[14] H.C. Shin, W.I. Cho, H. Jang, Electrochim. Acta 52 (2006) 1472.
[15] I. Belharouak, C. Johnson, K. Amine, Electrochem. Commun. 7 (2005) 983.
[16] J.-K. Kim, J.-W. Choi, G. Cheruvally, J.-U. Kim, J.-H. Ahn, G.-B. Cho, K.-W. Kim, H.-J. Ahn, Mater. Lett. 61 (2007) 3822.
[17] M. Konarova, I. Taniguchi, Powder Technol. 191 (2009) 111.
[18] C.-Z. Lu, G.T.-K. Fey, H.-M. Kao, J. Power Sources 189 (2009) 155.
[19] H. Joachin, T.D. Kaun, K. Zaghib, J. Prakash, J. Electrochem. Soc. 156 (2009) A401.
[20] Y. Zhang, H. Feng, X. Wu, L. Wang, A. Zhang, T. Xia, H. Dong, M. Liu, Electrochim. Acta 54 (2009) 3206.
[21] G.T.-K. Fey, T.-L. Lu, J. Power Sources 178 (2008) 807.
[22] C.R. Sides, F. Croce, V.Y. Young, C.R. Martin, B. Scrosati, Electrochem. Solid-State Lett. 8 (2005) A484.
[23] Y. Xu, Y. Lu, L. Yan, Z. Yang, R. Yang, J. Power Sources 160 (2006) 570.
[24] K. Wang, R. Cai, T. Yuan, X. Yu, R. Ran, Z. Shao, Electrochim. Acta 54 (2009) 2861.
[25] S.L. Bewlay, K. Konstantinov, G.X. Wang, S.X. Dou, H.K. Liu, Mater. Lett. 58 (2004) 1788.
[26] M.-R. Yang, T.-H. Teng, S.-H. Wu, J. Power Sources 159 (2006) 307.
[27] A. Yamada, S.C. Chung, K. Hinokuma, J. Electrochem. Soc. 148 (2001) A224.
[28] B. Kang, G. Ceder, Nature 458 (2009) 190.
[29] M. Koltypin, D. Aurbach, L. Nazar, B. Ellis, J. Power Sources 174 (2007) 1241.

[30] D. Choi, P.N. Kumta, J. Power Sources 163 (2007) 1064.
[31] K. Dokko, K. Shiraishi, K. Kanamura, J. Electrochem. Soc. 152 (2005) A2199.
[32] G. Meligrana, C. Gerbaldi, A. Tuel, S. Bodoardo, N. Penazzi, J. Power Sources 160 (2006) 516.
[33] I. Bilecka, A. Hintennach, I. Djerdj, P. Novak, M. Niederberger, J. Mater. Chem. 19 (2009) 5125.
[34] H. Yang, X.-L. Wu, M.-H. Cao, Y.-G. Guo, J. Phys. Chem. C 113 (2009) 3345.
[35] G.T.-K. Fey, Y.G. Chen, H.-M. Kao, J. Power Sources 189 (2009) 169.
[36] J.-K. Kim, G. Cheruvally, J.-H. Ahn, G.-C. Hwang, J.-B. Choi, J. Phys. Chem. Solids 69 (2008) 2371.
[37] H.-C. Kang, D.-K. Jun, B. Jin, E.M. Jin, K.-H. Park, H.-B. Gu, K.-W. Kim, J. Power Sources 179 (2008) 340.
[38] S. Lim, C.S. Yoon, J. Cho, Chem. Mater. 20 (2008) 4560.
[39] C.M. Doherty, R.A. Caruso, B.M. Smarsly, C.J. Drummond, Chem. Mater. 21 (2009) 2895.
[40] I. Taniguchi, Mater. Chem. Phys. 92 (2005) 172.
[41] K. Zaghib, J.B. Goodenough, A. Mauger, C. Julien, J. Power Sources 194 (2009) 1021.
[42] I. Taniguchi, C.K. Lim, D. Song, M. Wakihara, Solid State Ionics 146 (2002) 239.